Identifying local vs. regional drainage using multiproxy provenance tracers
Tracking the Moroccan Late Triassic fluvial system

Lovell-Kennedy, James; Roquette, Emmanuel; Schröder, Stefan; Charton, Remi; Redfern, Jonathan

DOI
10.1016/j.jafrearsci.2023.104866

Publication date
2023

Document Version
Final published version

Published in
Journal of African Earth Sciences

Journal of African Earth Sciences 200 (2023) 104866

Contents lists available at ScienceDirect

Journal of African Earth Sciences

journal homepage: www.elsevier.com/locate/jafrearsci

Identifying local vs. regional drainage using multiproxy provenance tracers – Tracking the Moroccan Late Triassic fluvial system

James Lovell-Kennedy [a,b,*], Emmanuel Roquette [a], Stefan Schröder [a,b], Remi Charton [a,c], Jonathan Redfern [a,b]

[a] North Africa Research Group, UK
[b] The University of Manchester, UK
[c] TU Delft, the Netherlands

ARTICLE INFO

Handling Editor: Dr Mohamed Mohamed G Abdelsalam

Keywords:
Triassic
Pangea
Rifting
Provenance
Heavy minerals
Petrography
Paleogeography

ABSTRACT

The Kerrouchen Basin is an understudied rift basin in the Middle Atlas of Morocco, where over 600 m of Triassic stratigraphy is well exposed. It was partially inverted during the Atlasic orogeny whilst preserving the original basin geometry. Within the Kerrouchen Basin, two distinct fluvial systems are present. The first, recorded by the K3 Formation, is a braided-meandering fluvial system showing vertical and lateral amalgamation. The K3 is an axial fluvial system that shows a predominant drainage direction towards the north-north-east, parallel to the rift zone axis, ultimately draining towards the Tethys Ocean. The K4 Formation records a secondary, Tributary Fluvial System (TFS), with facies spanning a range of alluvial-fluvial processes. Paleoflows predominantly record drainage to the SSW, transverse to the basin axis.

Heavy mineral and petrographic analysis of the two fluvial systems indicates two distinct sedimentary provenances for the depositional system. The K3 system records a higher proportion of sediment sourced from igneous rocks. In contrast, the K4 system records a local provenance signal derived from adjacent low-medium grade metamorphic terranes exposed to the east. Comparison of the provenance and stratigraphic trends within the Kerrouchen Basin with work undertaken in the Central and Western High Atlas suggests a shared source region for the through going axial fluvial systems recorded in the High Atlas and Kerrouchen basins. Our study provides evidence for a linked fluvial system spanning the High and Middle Atlas rifts during the Triassic, indicating that a regional fluvial system was present within Central Pangea from Middle-Late Triassic times. Identifying regional and local drainage networks within the Triassic rift basins has key implications for paleogeographic reconstructions and future exploration efforts for hydrocarbons and CCS sites within Morocco.

1. Introduction

Recent discoveries within the Triassic of the Tendrara – Missour Basin have renewed interest within the continental fluvial-aeolian Triassic sandstones which form voluminous reservoirs across North Africa (Acheche et al., 2001; Galeazzi et al., 2010, 2012; Macgregor, 1998). The latest oil and gas exploration efforts across North Africa have targeted the Triassic fluvial-aeolian play (the Trias Argilo-Gréseux Inférieur – TAG-I), which has been highly productive across Algeria, Libya and Tunisia. Development and evaluation of these discoveries has been hampered by highly heterogenous reservoir units and poor understanding of sediment fairways within the rift basins. These uncertainties can only be addressed with (1) improved understanding of the range of sedimentary facies within Triassic rift basins and (2) constraining the extent and scale of Triassic depositional systems on a regional to basinal scale.

Within the southern Middle Atlas Kerrouchen Basin Triassic fluvial outcrops are exposed, enabling sedimentological analysis to characterise the range of sedimentary facies which may be expected within a Triassic rift basin, similar to previous studies in Morocco (Bouabdelli and Piqué, 1996; Courel et al., 2003; El Arabi et al., 2003; Fabuel-Perez et al., 2009; Mader et al., 2017; Mader and Redfern, 2011; Olsen et al., 2000; Oujidi et al., 2006) the Atlantic conjugate margin (Houten and Van Houten, 1977; Leleu et al., 2016; Leleu and Hartley, 2010) and across North Africa (Bourquin et al., 2010; Sabaou et al., 2005; Soussi et al., 2017; Turner et al., 2001). To supplement this work, a multi-proxy provenance

* Corresponding author. North Africa Research Group, UK.
E-mail address: james.lovell-kennedy@manchester.ac.uk (J. Lovell-Kennedy).

https://doi.org/10.1016/j.jafrearsci.2023.104866
Received 12 July 2022; Received in revised form 2 February 2023; Accepted 2 February 2023
Available online 9 February 2023

analysis was utilised in order to constrain the source of the depositional systems, and therefore the scale of the source-to-sink system.

The result of the provenance analysis were then integrated with previous thermochronology studies from across the Anti-Atlas (Gouiza et al., 2017), the High Atlas (Domènech et al., 2016) and the Moroccan Meseta (Barbero et al., 2011; Saddiqi et al., 2009) and detrital zircon U–Pb geochronology to assess the provenance of the sands found within the Central High Atlas basins (Domènech et al., 2018; Marzoli et al., 2017; Perez et al., 2019). Integrating the new sedimentological and multi-proxy provenance data from this study with the previously published work has enabled us to propose a new depositional and paleogeographic model for both the Kerrouchen Basin and northern Morocco during the Middle - Late Triassic rifting and early Pangea break up.

2. Geological setting

The Moroccan Triassic is known from outcrop in the Argana Valley, the Central High Atlas and the Middle Atlas, with Triassic sediments also preserved in the subsurface of the Tendrara – Missour Basin to the east and the Essaouira – Sous Basin to the west, and along the Moroccan Atlantic Margin (Fig. 1) (Baudon et al., 2009; Beauchamp, 1988; Beauchamp et al., 1996; Bouabdelli and Piqué, 1996; Cousminer and Manspeizer, 1976; El Arabi et al., 2003; Ellouz et al., 2003; Escosa et al., 2021; Fabuel-Perez et al., 2009; Hafid, 2000; Houten and Van Houten, 1977; Laville et al., 1995, 2004; Laville and Petit, 1984; Mader et al., 2017; Mader and Redfern, 2011; Redfern et al., 2010). The Triassic forms a continental syn-rift mega-sequence, unconformably overlying the Variscan unconformity surface, infilling a series of extensional grabens and half-grabens which formed during the early breakup of the Pangean supercontinent (Fig. 1) (Brown, 1980; Houten and Van Houten, 1977; Laville and Petit, 1984; Mattis, 1977).

2.1. Tectonic overview

The Early Mesozoic sequences of Morocco record the initial break-up of the Pangean supercontinent, which led to the opening of the Atlantic Ocean to the west and Tethys to the north-east, as well as the development of rift basins across Morocco (Veevers, 1994). Beginning in the late Permian to Early Triassic, post Variscan orogenic collapse and associated crustal thinning occurred along the future Atlantic margin, with intra-montane rifts (Baudon et al., 2012; 2009) and rift shoulder uplift occurred in the Anti-Atlas (Ruiz et al., 2011). Significant strike slip tectonics predominated in the Middle Triassic along major E-W trending shear zones; the South Atlas Fault (SAF) and the Azores-Gibraltar Fracture Zone (AGFZ) (Laville et al., 2004, 1995; Laville and Petit, 1984; Piqué et al., 1998; Sahabi et al., 2004; Schettino and Turco, 2009).

Renewed extension, driven by the opening of the proto-Atlantic in Late Triassic times led to a series of broad rift basins, which accumulated up to 5000 m of sediment (Leleu et al., 2016; Mader et al., 2017; Mader and Redfern, 2011). Rifting was commonly focused along structures inherited from the Variscan orogenic cycle, with a peak in rifting during the Carnian period, and a quiescence during the Norian-Rhaetian (Domènech et al., 2018; 2015; Laville et al., 2004; Ouarhache et al., 2000).

A final pulse of tectonic activity resulted in continental break-up in the latest Triassic to early Jurassic times (Rhaetian – Hettangian), leading to the eruption of the voluminous tholeiitic basalts of the Central Atlantic Magmatic Province (CAMP basalts) (Fiechtner et al., 1992; Marzoli et al., 2004; Olsen et al., 2000; Schlische et al., 2013; Verati et al., 2007; Whiteside et al., 2007). Across Morocco, this volcanic event was associated with a significant strike-slip or normal rifting component (Laville and Petit, 1984; Ouarhache et al., 2012; Piqué et al., 1998).

2.2. The Kerrouchen Basin

The Kerrouchen Basin is a partially inverted Mesozoic rift basin with significant Triassic outcrop along the Oued Srou River and its tributaries, with the original basin geometry preserved (Lachkar et al., 2000; Laville et al., 1995, 2004; Lorenz, 1976; Ouarhache et al., 2000, 2012) (Fig. 2). The Kerrouchen Basin is situated at the south of the Middle Atlas rift, between two distinct Palaeozoic terranes. To the east, Palaeozoic basement forms part of the Inner Eastern Zone (Midelt Zone) which underwent deformation during the end Devonian – early Carboniferous at ca. 360 Ma (Hoepffner, 1987; Hoepffner et al., 2005, 2006). To the west is the Azrou-Khenifra zone of the intermediate zone of the Moroccan Variscan belt, which underwent Visean deformation prior to

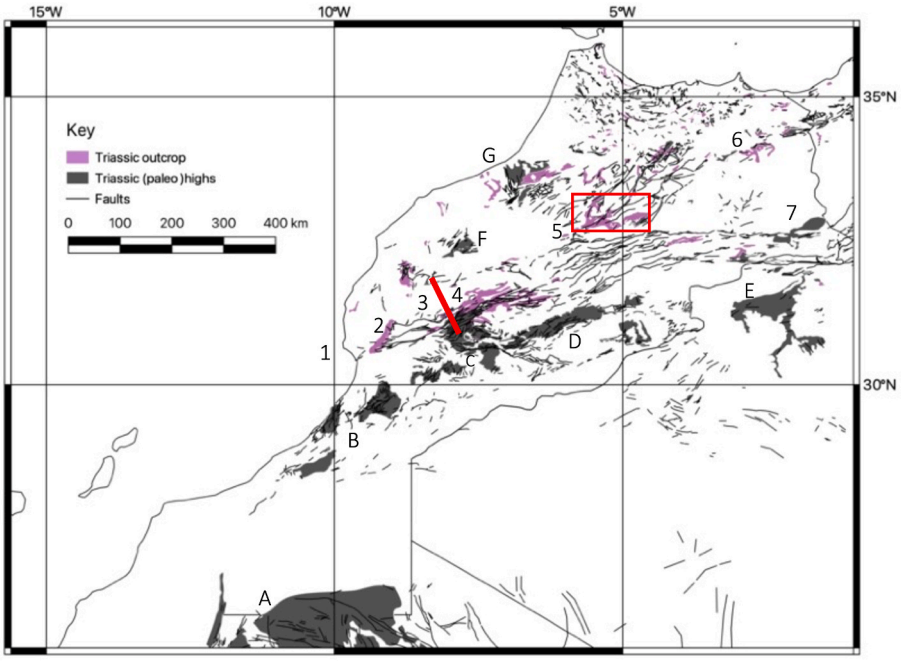

Fig. 1. Map of northern Morocco, with Triassic outcrop (purple) and Triassic paleohighs identified via thermochronology studies (Barbero et al., 2007; Charton et al., 2021, 2018; Domènech et al., 2018; Gouiza et al., 2019, 2017; Lafforgue, 2016, chap. 4; Oukassou et al., 2013; Saddiqi et al., 2009). Map based on geological map of Morocco, digitised within the NARG GIS Database. Red box indicates Kerrouchen basin, the focus of this study. Numbered regions indicate Triassic Basins, from east to west, (1) Essaouira basin (subsurface and offshore), (2) Argana Valley (3) Tizi-n-Test (4) Oukaïmeden (5) Kerrouchen Basin (6) Oujda Mountains (7) Tendrara – Missour Basin (subsurface). Labelled regions indicate potential source regions based upon thermochronology studies, from North to South, (A) The Reguibat Shield (B) the Western Anti-Atlas (C.) Central Anti-Atlas (D) Eastern Anti-Atlas (E.) Boarfa Region (F) Jebilet Massif (G) Zaer Massif. A key feature of the Triassic of Morocco is a marked divide in paleoflows within the Central High Atlas between the Tizi-n-Test (3) and the Oukaïmeden Basin (4), marked by a red line. Paleoflows flow to the west in the Tizi-n-Test and Argana Valley and towards the east in the Oukaïmeden Valley (Ellouz et al. 2003).

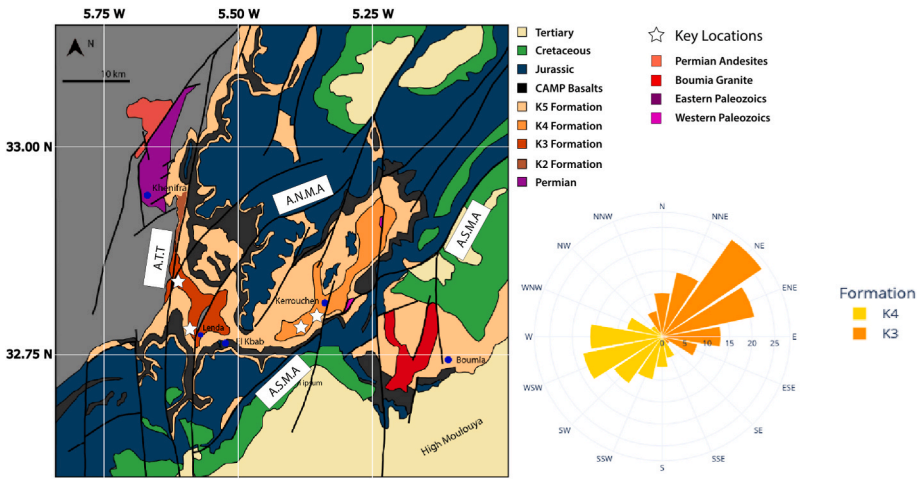

Fig. 2. High detail map of the Kerrouchen Basin (left) and Triassic paleoflows (right). Key faults controlling evolution of the Middle Atlas rift basin are labelled. ATT = Accident Tizi n'Trettene, ANMA = Accident Nord Moyen Atlas, ASMA = Accident Sud Moyen Atlas. The K3 formation primarily outcrops near the Lenda village, along the A.N.M.A. Paleoflows within the K3 formation primatily flow towards the NE. The K4 formation primarily outcrops in the east of the basin, with paleoflows towards the WSW and SW. This indicates the K4 formation was eroding into uplifted footwall scarps along the ASMA fault system, which marks the eastern basin boundary.

being thrust west and refolded during the Permian (Allary et al., 1972; Bouabdelli and Piqué, 1996; Hmich et al., 2006; Ntarmouchant et al., 2016).

Between these two contrasting basement domains lies the Kerrouchen Basin, limited to the east by the 'Accident Sud Moyen Atlasique' (ASMA) and to the west by the 'Accident Tizi n'Trettene (ATT) (Ouarhache et al., 2012). These major faults strike ~ N40, were inherited from the Variscan Orogeny and were important during the Upper Triassic rifting which formed the Middle Atlas Rift (Laville et al., 1995, 2004).

The Kerrouchen Triassic Formations record a polyphase rift evolution. Initial rifting occurred during the Carnian along inherited Variscan faults leading to Formation of a broad, asymmetric half-graben infilled by conglomerates (K2 Formation), fluvial sandstones (K3 and K4 Formations) (Laville et al., 2004; Ouarhache et al., 2012). During the Norian, sabkha type mudstones formed across the basin (K5 Formation), recording a dampening of the fault activity within the late Triassic post-rift phase (Lachkar et al., 2000; Laville et al., 2004; Ouarhache et al., 2012). Tectonic activity renewed during Rhaetian times, with transtensive or extensional tectonics leading to the eruption of 100–200 m thick basalts across the basin, linked to the CAMP event (Fiechtner et al., 1992; Laville and Petit, 1984; Ouarhache et al., 2000). This second rift phase was followed by a secondary post-rift phase in the Liassic, with marine carbonates forming across the Middle Atlas rift, recording the Tethyan transgression during the early Jurassic.

3. Sedimentology

3.1. Facies analysis

The sedimentology of the Triassic Formations of the Kerrouchen Basin has been analysed and grouped into facies associations, made of lithofacies (Table 1) defining depositional environments. There are four principal facies associations identified within the Kerrouchen Basin: (1) Alluvial Fan Facies (FA-1), (2) Alluvial – Fluvial Fan Facies (FA-2), (3) Channel Facies (FA-3) and (4) Overbank Facies (FA-4).

3.1.1. FA-1: Alluvial Fan Facies association

Facies association FA-1 consists of 0.3–20 cm thick units which can be traced up to a 100 m parallel to paleoflow direction. Internal beds range from 0.3 to 10 m thick. The units exhibit a sharp to concave up base, beginning with red, friable conglomerates. FA-1 is comprised of two lithofacies – the conglomeratic lithofacies Gms-b and the mudstone facies Fm.

The conglomeratic Gms-b lithofacies displays a range of grainsizes, from very coarse sand to very large pebbles within a sandy matrix. Clasts are both intrabasinal (red mudstones and sandstones) and extrabasinal (limestones, granites, quartz, schist and phyllites). Sedimentary structures are rare, with crude clast imbrication, fining up trends and erosive basal contacts.

In the east of the basin, FA-1 reaches maximum thickness of 2–5 m. In the west of the basin a maximum thickness of up to 20 m is observed. FA-1 is limited to marginal settings in the basin and intra-basinal highs of Palaeozoic basement into which it erodes.

Interpretation: FA-1 is interpreted to record hyper-concentrated flows with high sediment to water ratios deposited within alluvial fans in rift settings (Mack and Leeder, 1999; Miall, 2013). The geographic extent of FA-1 indicates these alluvial fans were sourced from local basement highs, exposed in footwall highs during Triassic rifting.

3.1.2. FA-2: alluvial – fluvial fan facies association

Facies association 2 is comprised of three major sedimentary facies; FA-2A, 2 B and 2C, displayed in Figs. 6 and 7.

3.1.2.1. FA-2A: proximal alluvial-fluvial fan facies association. FA-2A comprises two principal lithofacies; lithofacies St and lithofacies Sh. Lithofacies St is poorly sorted; with coarse grained sand to granular grade within a clast supported matrix. It is marked by concave up erosive bases which are overlain by erosive lags.

It forms 10–15 m thick units, capped by mudstones, which can be traced for several hundred metres along depositional strike. FA-2A is limited to outcrops near the town of Kerrouchen within the west of the basin, where it outcrops in the vicinity of fault relay zones along the basin bounding fault, the ASMA.

Within the beds, wide (up to 20 m), concave geometries can be observed. Sedimentary structures within lithofacies St are predominantly trough cross-beds with rare planar cross-bed sets. Beds show a clear fining-up trend from granular basal lags to medium-coarse grained sand. The erosive lags contain extra formational clasts of feldspathic and metamorphic composition, alongside intra-formational clasts of sandstone, mudstones and paleosol fragments.

Lithofacies Sh consists of well sorted, matrix supported, fine to medium grained sand. It is organised into sharp based beds up to 25 cm thick. This facies displays horizontal lamination, although locally planar crossbedding is observed. Within FA-2A, lithofacies Sh is typically laterally discontinuous and eroded out by overlying beds of lithofacies St.

Interpretation: Lithofacies St is interpreted to have been deposited following erosion and abandonment of confined channels, with rapid deposition of a poorly sorted bedload above an erosive surface. The vertical and lateral amalgamation of the beds to form distinct units was driven by vertical and lateral aggradation during channel migration.

Table 1
Lithofacies table.

Lithofacies code	Lithology	Sedimentology	Environment of Deposition
Gms – b	Red, friable conglomerates with poorly sorted, granule to coarse pebble grade, angular to sub-rounded, matrix to clast supported. Extraforaminal and intraformational clasts: red mudstones, red sandstones, limestones, granitic fragments, vein quartz, schistose fragments, and slate fragments.	Very thick to thick, massively to crudely bedded, with erosive basal scours Rare internal structures include clast imbrication. Crude fining up trends are locally observed. Onlap and erode into paleo-highs of Hercynian basement	Alluvial fan debris flow deposits
Gt	Poorly cemented grey conglomerates consisting of poorly sorted, angular to sub-rounded pebbles within a medium-coarse sand matrix. Extraforaminal and intraformational clasts: red mudstones, red sandstones, limestones, granitic fragments, vein quartz, schistose fragments, and slate fragments. Metamorphic and igneous rock fragments are more common in the east of the basin, with sedimentary fragments more common in the west of the basin.	1–2 m deep, cross-cutting channel bodies with erosive basal scours Channels display a fining up trend Massive to crude laminations or low angle to horizontal bedding present within the upper part of the channel complexes. Commonly, the channels erode into paleosol horizons.	Gravelly braided fluvial system
St	Granular to v. coarse grade, clast supported sand. Poorly sorted. Feldspathic and metamorphic lithic fragments.	Thick beds (0.3–3 m), with large scale channel (>10 m width) bodies, with erosive bases and lags containing reworked palaeosols and mudstone fragments. Sedimentary structures include trough crossbedding, large- and small-scale cross-beds. Beds display normal grading.	Sandy braided fluvial system
Sr	Granular to v. coarse sand grade, clast supported sandstone. Moderate to well sorted.	Thin to thickly bedded, with erosive bases and sharp tops, forming wide (3–5 m) channels. Sedimentary structures include planar and trough crossbedding and low angle to horizontal lamination near the top of beds.	Meandering fluvial system
Sp	Red, rounded-sub angular, coarse to medium grade, matrix supported sandstones. Moderate to well sorted.	Thickly bedded sandstones containing channel bodies and lateral accretion surfaces. Moderate fining up trend. Sedimentary structures are dominated by planar cross-bed sets.	Meandering fluvial system
Sl	Red, well sorted, sub-rounded to rounded, medium grade, matrix supported sandstones. The matrix is locally calcerous and contains white, gypsum streaks.	Thin to thickly bedded sandstones with sharp tops and occasional erosive bases. Fining up trend present. Sedimentary structures include low-angle cross-beds, planar cross-bedding, trough cross bedding and flaser bedding.	Ephemeral fluvial – tidal facies.
Sh	Red, well sorted, sub-rounded-rounded, matrix supported, fine-medium grade sand.	Medium to thinly bedded tabular sandstones. Beds contain low angle to horizontal laminations. Alternate with mudstones, but locally stack. Where stacked, contain planar cross-bedding	Crevasse splay deposits
Fm	Red siltstones containing thin paleosols and calcretes	Structureless	Overbank deposits
Fsc	Red mudstones, locally containing gypsum dolomitic rhombs	Structureless	Overbank fines/ sabkha mudstones

Lithofacies Sh represents deposition of an unconfined flow, indicating deposition within a crevasse splay upon a fluvial floodplain.

Combining the architecture of the fluvial bodies and the lithofacies FA-2A is interpreted to be situated within the proximal zone of an Alluvial – Fluvial fan type system (Nichols and Fisher, 2007).

3.1.2.2. FA-2B: medial alluvial-fluvial fan facies association. FA-2B consists of three principal lithofacies: Gt, Sh and Fm. FA-2B forms 5–10 m thick units with internal beds ranging from 0.1 to 3 m thick. The units form laterally continuous outcrops which can be traced for up to a hundred meters.

Lithofacies Gt forms comprises poorly sorted, angular to sub-rounded pebbles within a medium-coarse sand grade matrix, displaying a vertical trend from massive bedding to parallel to low-angle laminations present within the upper part of the bed. It is deposited within thick to very thick beds, 1 – 3 m, with concave bases. Bed tops are usually sharp but can be eroded into by overlying beds of lithofacies Gt, that form channel geometries. Each unit is comprised of multistorey and multilateral small (2 – 5 m wide) channel fills, with maximum thickness of approximately 0.4 m, which extend laterally for up to 100 m.

Lithofacies Sh is sedimentologically similar in both proximal and medial settings, although its architecture is different. The sedimentology consists of well sorted, matrix supported, fine to medium grained sand. It is organised into sharp based beds up to 25 cm thick. This facies displays horizontal lamination, although locally planar crossbedding is observed. Within FA-2B, lithofacies Sh forms more laterally, sheet like, continuous beds, where it overlies lithofacies Gt.

Lithofacies Fm is a massive, structureless mudstone ranging in thickness from 1 to 10 m. Units of lithofacies Fm sharply overlie the underlying gravelly and sand rich facies, increasing in thickness towards the basin centre. Laterally, the gravelly lithofacies (Gt) and sandy lithofacies (Sh), grade into the mud-rich lithofacies (Fm) on scales of up to 100 m. Locally, palaeosols are observed at the top of the units of lithofacies (Fm).

3.1.2.2.1. Interpretation. Lithofacies Gt is interpreted to have been deposited within minor channels of a gravelly fluvial system. Lithofacies Sh is interpreted to have formed as crevasse splay deposits on a fluvial floodplain during flood events, with lithofacies Fm representing background deposition of overbank fines on the floodplain.

The thin, laterally amalgamated channels of lithofacies Gt, overlain by the sheet like sands of lithofacies Sh, which grade laterally and vertically into the overbank lithofacies Fm are typical of the medial zone of the alluvial – fluvial fan type system (Nichols and Fisher, 2007).

3.1.2.3. FA-2C: distal alluvial – fluvial fan facies association. Facies association FA-2C consists of two lithofacies, lithofacies Sh and Fm. Within

FA-2C, lithofacies Sh forms laterally continuous, thin, sheet like sand bodies dominated by low-angle (<10°) crossbedding. Lithofacies Fm thickens towards the basin centre, separating isolated beds of lithofacies Sh.

Interpretation: FA-2C represents distal, alluvial – fluvial fan facies. The thin, sheet like nature of lithofacies Sh likely represent terminal crevasse splays (Nichols and Fisher, 2007).

3.1.3. FA-3: Channel Facies Association

Facies Association FA-3 is comprised of three sand-rich lithofacies (Sr – Sp – Sh) and the gravelly lithofacies Gt, predominantly exposed near the village of Lenda, within the west of the Kerrouchen Basin, displayed in Figs. 3–5.

3.1.3.1. FA-3A: meandering fluvial system. Facies association FA-3A consists of three sand-rich lithofacies: Sr – Sp – Sh.

Lithofacies Sr consists of red, very coarse-grained clast-supported sand overlying concave up bases. Lithofacies Sr is vertically amalgamated to form multi-storey channel fill complexes up to 10–15 m thick, with individual beds ranging from 1 to 3 m in thickness. Bed tops are sharp, although they can be cut into by overlying beds. Sedimentary structures include trough cross-bedding and steep (>10°) and low-angle (<10°) planar crossbedding. Weak grading is present, with individual beds showing subtle fining-up trends.

Lithofacies Sp is moderately well sorted, coarse-medium grained sand, dominated by high-angle (>10°) planar crossbedding, within beds that have flat to shallow, concave-up basal surfaces, defining units which reach up to 1 m in thickness.

Within FA-3A, lithofacies Sh forms thin sheet-like sandstones which are interbedded with, and laterally amalgamated with, lithofacies Sr and Sp.

Interpretation: The three lithofacies unique to FA-3 (Sr, Sp and Sl) represent various elements within a fluvial system. Lithofacies Sr is interpreted to be fluvial bars formed in downstream or mid-channel accretion typical of a sandy braided fluvial system. Lithofacies Sp is interpreted to record transverse bars within a sandy fluvial system. Lithofacies Sl is interpreted to represent deposition in an environment with alternating periods of fast-moving and slack water, interpreted here as a evidence of development of more ephemeral fluvial styles (Martin, 2000).

3.1.3.2. FA-3B braided fluvial system. FA-3B consists of three lithofacies, Gt, Sh and, locally, FSc.

Lithofacies Gt consists of poorly cemented grey-red conglomerates consisting of poorly sorted, angular to sub-rounded pebbles within a medium-coarse sand matrix. The gravelly conglomerates form 0.3–1.5 m thick beds, with concave up-surfaces at the base overlain by larger clasts. The beds fine up, with gravel sized fragments more common at the base and matrix more common at the top of beds, where low-angle cross bedding can be observed. Within the coarser basal lags, a range of clast types can be observed, including fragments of lithofacies Fsc and Sh, paleosol fragments and sedimentary clasts thought to be from older, Palaeozoic units.

Within FA-3B, lithofacies Gt are associated with lithofacies Sh, which consists of well-sorted sandstones forming laterally continuous, thin, sheet like sand bodies dominated by laterally or low-angle (<10°) crossbedding. Lithofacies Sh is often overlain by Lithofacies Fsc, which can form beds of up to 0.3 m, although typically thinner beds are observed.

Interpretation: Facies association FA-3B is interpreted to represent deposits of a gravelly-braided stream system. Lithofacies Gt represents major channels, overlain by flashflood or sand flat deposits of lithofacies of Sh and Fm. The presence of palaeosols in the erosive scours could be indicative of ephemeral flow.

3.1.4. FA-4 overbank facies association

FA-4 is comprised primarily of lithofacies Fsc, a fine-grained lithofacies, and the coarser-grained lithofacies Sl and Sh.

Lithofacies Sh forms laterally continuous, thin, sheet like sand bodies dominated by laterally or low-angle (<10°) crossbedding. Lithofacies Sl consists of sharply based red sandstones, with well sorted, sub-rounded to rounded, medium grain sand in a mud rich, calcareous matrix. Lithofacies Sl forms isolated, thin to medium (0.1–0.3 m) thick beds and is associated with the mud-rich lithofacies Fsc. A wide array of sedimentary structures are present within lithofacies Sl, including low-angle (<10°) planar cross-bedding, trough cross-bedding, climbing ripples and flaser bedding (Figs. 4 and 5).

Lithofacies Fsc forms massive structureless mudstone units which form the majority of outcrop within the Kerrouchen Basin. Locally, gypsum and calcretes can be observed within the red mudstones, and a local halite mine is believed to be present within this facies (Lorenz, 1976). Lithofacies Fsc is lateral to and overlying coarser grained, sandy, and gravelly lithofacies.

Interpretation: Lithofacies Fsc is interpreted to be overbank mudstones deposited on a fluvial floodplain locally underwent evaporation.

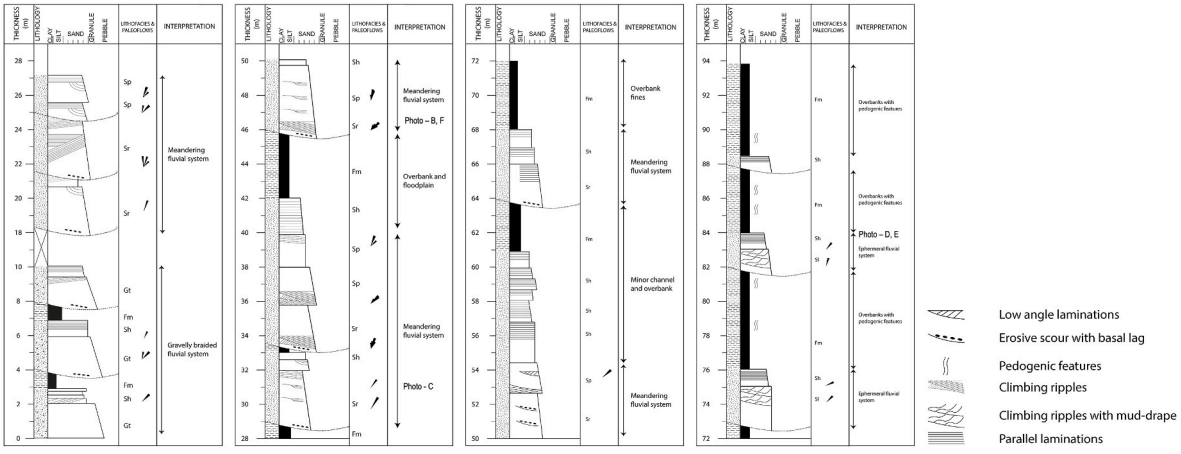

Fig. 3. Composite log of the K3 formation from the Lenda village locality (32.769281N, -5.573660). At this locality, a general fining up trend is displayed, with gravelly braided fluvial systems passing into a sandy braided fluvial system which dominates the stratigraphy. The upper section records a decrease in fluvial energy and development of more extensive, stable overbanks, potentially linked to a sabkha or lacustrine type setting. The paleoflows throughout the unit are consistent, with drainage orientated between NNE and ENE throughout.

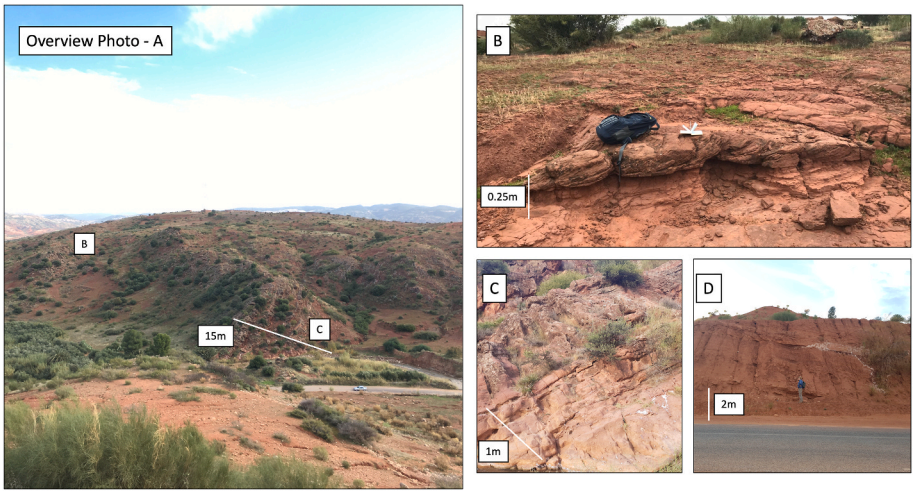

Fig. 4. Field images of the K3 formation, outcropping near Lenda Village (32.769281, −5.573660). Photo A is taken looking north, with the location of photo B and C indicated. Photo B displays a channel body showing lateral accretion surfaces. Photo C displays a series of vertically amalgamated channel bodies from the Channel Facies Association, FA-3. Photo D shows beds from the upper section, where sheet like geometries, climbing ripples and flaser bedding occur, of Lithofacies Sl interbedded with Lithofacies FSc, deposited during flood events on the floodplain.

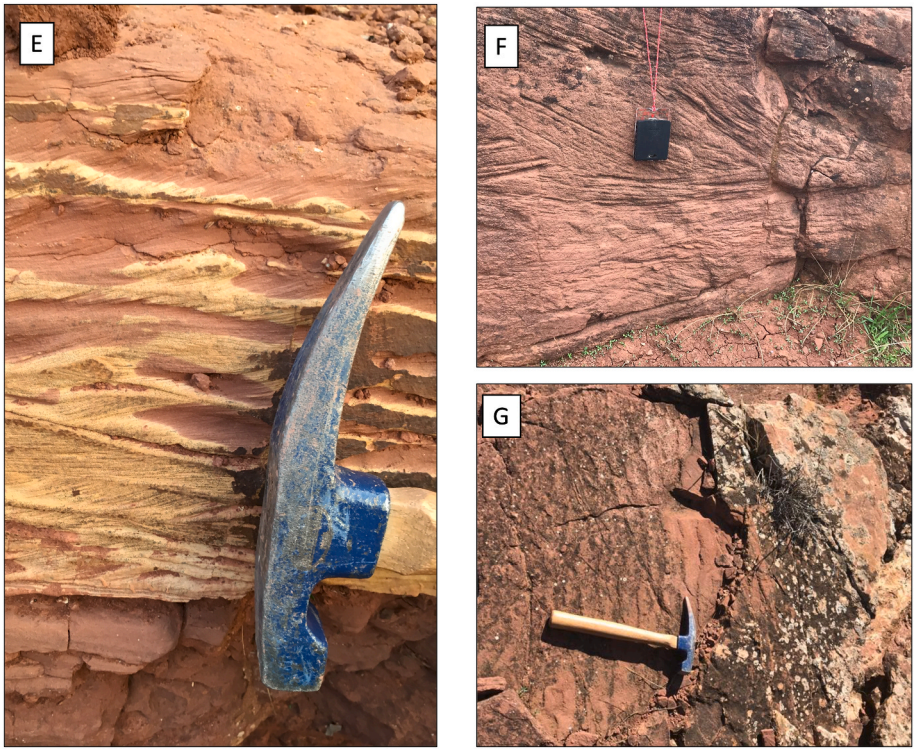

Fig. 5. Photos of the K3 formation. Photo E displays climbing ripples from the upper part of the section, with F and G displaying cross-bedding and ripples from lower in the section. Locations of the photos can be seen on the log in Fig. 3.

4. Facies distribution

The distribution of the facies associations across the Kerrouchen Basin allows for the identification of several distinct sedimentary systems.

Firstly, the K2 Formation is dominated by coarse grained conglomerates deposited on alluvial fans eroded from the underlying basement units. The alluvial fan conglomerates are unconformably overlain by the mudstones of the K5 Formation. The alluvial fans record paleoflows towards the basin centre, with flow to the east along the western boundary and the east along the eastern basin boundary.

The K3 and K4 Formations outcrop in the west and east of the basin respectively. In the west, the K3 Formation outcrops near the village of Lenda, where a range of fluvial facies typical of a meandering style fluvial system are exposed, with laterally equivalent mudstones. The dominant facies present are the channel facies (FA – 3 A) and overbank facies (FA-4), with subordinate examples of braided fluvial style (FA-3B) (Fig. 3). Paleoflows within the K3 Formation range from ESE to NNW, show a predominant trend towards the NNE, parallel to sub-parallel to the three major rift faults which controlled the opening and inversion of the Kerrouchen Basin (Fig. 2).

In the east of the basin, the K4 Formation outcrops near the town of Kerrouchen and along the Oued Srou Valley. Near Kerrouchen, large sandstone ridges expose proximal alluvial – fluvial fan facies (FA-2A) and braided-stream facies (FA-3A), which pass to medial (FA-2B) and distal facies (FA-2C) to the west, south and north, with mudstones proportion increases in prominence to the south, west and north (Fig. 6). The K4 formation passes into the overbank facies association (FA-4) near

the town of El Kbab (Fig. 2) Paleoflows within the K4 Formation range from SSE to NNW but are predominantly SW to W (Fig. 2), indicating sediment was sourced from the west.

The combination of lithofacies and paleoflow analysis allows for the identification of three depositional systems within the Kerrouchen Basin. The first, the K2 Formation, represents local alluvial fans fringing and eroding into local basement highs. The overlying K3 Formation records a braided-meandering fluvial system, flowing broadly parallel to the rift axis. The distribution of facies within the K3 Formation is potentially controlled by tectonics, as much of the outcrop is along the ANMA fault, suggesting possible fault control capturing the fluvial system in the hanging wall, although outcrop distribution may limit further detailed field evidence to verify this. The K4 Formation records paleocurrent trends transverse to those recorded in the K3 Formation and to the main fault trends, which together with the clast composition suggests deposition within a tributary alluvial-fluvial system (TFS) flowing into the basin from uplifted regions along the eastern basin boundary, providing locally sourced sediment into the basin.

The identification of distinct depositional systems within the Kerrouchen Basin, the axial fluvial system in the K3 Formation and the transverse TFS systems in the K4 Formation, indicates that multiple source regions contributed to the fill of the Kerrouchen Triassic basin. To test this hypothesis and constrain the source of these systems, provenance analysis was used to discriminate between the sources of the Triassic depositional systems.

5. Provenance methods and results

Samples from within the K2, K3 and K4 Formation of the Kerrouchen Basin were selected for petrographic and heavy mineral provenance analysis.

5.1. Heavy mineral analysis

12 samples were selected for heavy mineral analysis from the K2, K3 and K4 Formations. Samples were disaggregated and wet sieved through a 250 μm sieve and a 32 μm sieve. The grains in the 250 μm–32 μm fraction were gravitationally separated in Lithium heteropolytungstate ($\rho = 2.80$ gcm-3) and recovered by partial freezing in liquid nitrogen. Heavy minerals were mounted onto grain mounts in epoxy resin for QEMSCAN (**Q**uantative **E**valuation of **M**inerals by **S**canning **E**lection **M**icroscopy). The SEM\QEMSCAN analysis was performed on a FEI Quanta 650 FEG SEM equipped with a Bruker Quantax EDS system. Data was collected at 15 kV accelerating voltage using a step size of 10 μm. Data processing was performed using the iDiscover software of the QEMSCAN system.

A compositional assignment is made for each acquisition point, allowing a compositional map of the sample to be generated. The iDiscover software outputs the results in a spreadsheet of volume percentages for each identified component, allowing for thousands of grains to be identified. QEMSCAN cannot identify polymorphs as it only looks at composition. Grains identified as Rutile (TiO_2) were checked using an optical microscope to confirm the compositional assignment. This method has limitations compared to other methods, such as Raman spectroscopy, as polymorph identification is limited to the skill of the user, though it has been used in similar studies e.g. Akinlotan et al., (2021).

Raw heavy mineral compositions are presented in appendix 1. The various indices were calculated using the equations in Table 2.

5.2. Petrographic analysis

16 thin section samples from sandstones within the Kerrouchen Basin K3 and K4 Formations were utilised for point counting. Samples were point counted using the ribbon method (Galehouse, 1971), with 400 grains identified using the Gazzi-Dickinson Method (Dickinson, 1970). Sedimentary grains were classified into quartz, feldspar or lithic fragments, with lithic fragments further classified into clastic (Ls), carbonate (Lc), metamorphic (Lm), volcanic (Lv) or plutonic (Lp) (Garzanti, 2016; Garzanti et al., 2010). The metamorphic grade of the lithic fragments was also recorded (Garzanti and Vezzoli, 2003). The resulting datasets were plotted into ternary diagrams. The parameters and results are given in Appendix 2.

6. Results

Petrographic analysis indicates the sandstones from the K3 and K4 Formations are lithic-arenites (12 samples) or sub-lithic-arenites (3 samples). A single sample from the K4 Formation was classed as a feldspathic lithic-arenite. Utilising the provenance discrimination outlined by Garzanti 2016), this indicates a recycled orogenic provenance for both the K3 and K4 Formations. The dominant lithic types vary between the two Formations (Fig. 8).

Within the K3 Formation, lithic fragments are dominated by clastic sedimentary (Lsp) or igneous (Lf) clasts. Metamorphic clasts (Lm) are rare and typically LM1 or LM2, i.e. very-low to low metamorphic grade (Garzanti and Vezzoli, 2003). In contrast, lithic fragments from the K4 Formation contain greater proportions of both metamorphic and igneous fragments, although sedimentary clasts are still the dominant clast type. The metamorphic clasts are typically higher grade; most belong to LM2 with some LM3 grains (low-medium metamorphic grade) (Garzanti and Vezzoli, 2003).

The heavy mineral assemblages are dominated by ultrastable heavy minerals, primarily Rutile ($\bar{x} = 30.0\%$) and Ilmenite ($\bar{x} = 28.3\%$). Hornblende and Apatite form significant populations ($\bar{x} = 20.0\%$ *and* 12.8% respectively), with Zircon ($\bar{x} = 5.9\%$) forming a

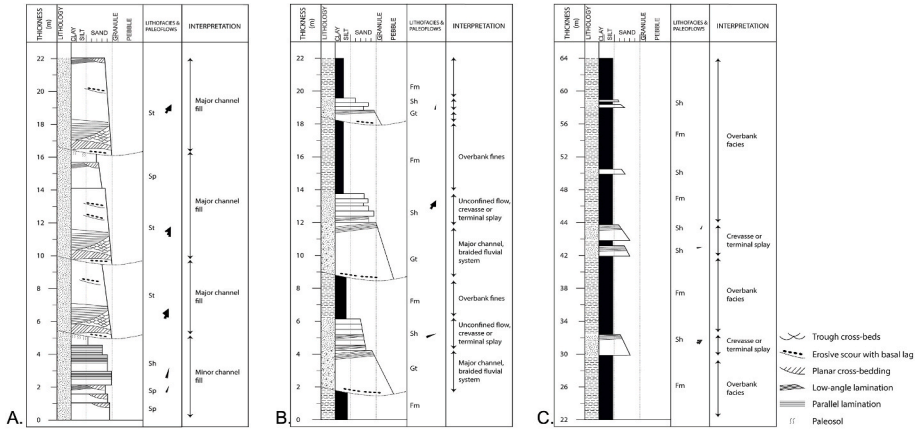

Fig. 6. Logs of the K4 formation from near the village of Kerrouchen. Log A indicates the typical proximal facies, best outcropping in the Kerrouchen Gorge (32.794353, -5.318671), which passes into the medial (B) and distal facies (C.) towards the WSW, exposed along the P7308 road, logged section at 32.77800419373195, -5.36561814554633. The paleoflows vary between S and W, but generally record drainage from uplift footwall regions towards the basin centre.

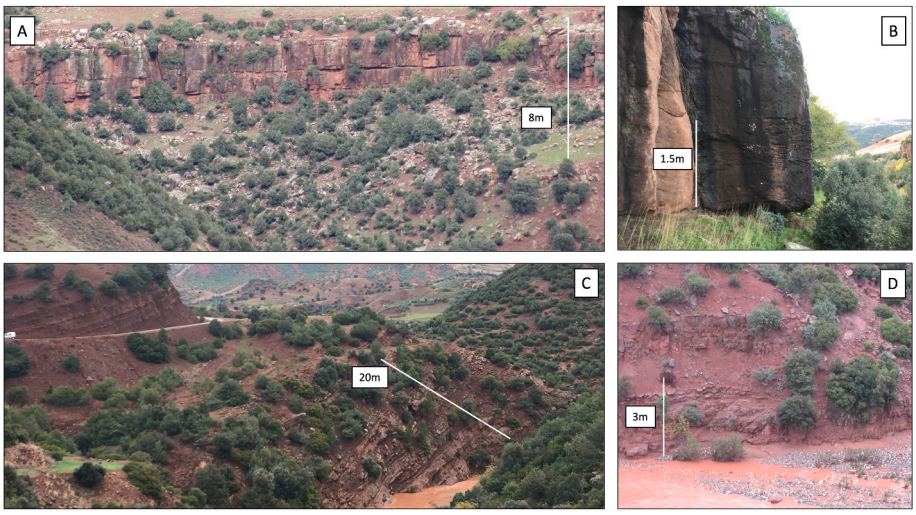

Fig. 7. Photos of the K4 Formation. Photos A and B are from the Kerrouchen Gorge ((32.794353, −5.318671), Photos B and C are from the logged section along the P7308 road (32.77800419373195, −5.36561814554633).

Table 2
Heavy Mineral Indices used within this study. The indices are from a range of previous studies. The Apatite-Tourmaline (ATi), Garnet-Zircon (GZi) and Rutile-Zircon (RZi) are from Morton and Hallsworth (1994). The Zircon – Tourmaline – Rutile index is from Hubert, 1962).

Indices	Calculation
ATi	Apatite%/(Apatite%+Tourmaline%)
GZi	Garnet%/(Garnet%+Zircon%)
RZi	Rutile%/(Rutile%+Zircon%)
ZTR	(Zircon% + Rutile% + Tourmaline%)

minor component. Amphibole, Clinopyroxene, Tourmaline and Garnet are all present as accessory populations ($\bar{x} <$ 2%) (Fig. 9).

The single sample from the K2 Formation from the eastern basin boundary contains elevated levels of hornblende ($\bar{x} =$ 34.3%) and tourmaline ($\bar{x} =$ 6%) compared to the basinal average. The K2 Formation also contains elevated levels of Garnet and Amphibole ($\bar{x} =$ 2.44% and 2.97 respectively), with lower proportions of rutile, zircon, and ilmenite.

The K3 Formation is defined by high levels of Rutile, Hornblende, Ilmenite, and Apatite, but displays a high degree of variability between samples. Hornblende varies from 4.8% to 56.4%, ilmenite from trace to 50%, rutile from 1.85% to 58% and apatite from 1% to 20%. Garnet, amphiboles and clinopyroxene remain low throughout (Figs. 10, 11 and 12). .

The variability within the K3 Formation has a stratigraphic component. Outcrops of both fluvial sands and overbank facies near the village of Lenda are characterised by very high levels of hornblende ($\bar{x} =$ 35%). Older outcrops of similar facies and lithofacies Sl to the south and west contain 10.6% hornblende on average. Apatite is also elevated in the Lenda outcrops (18.2% vs 8.2% for other K3 localities), with ilmenite, rutile and zircon reduced (14.0% vs 38.2%, 24.1% vs 33.5% and 2.6% vs 6.6%). The presence of relatively elevated levels of amphiboles and clinopyroxenes in this locality is also observed.

Within the K4 Formation there is no large changes in mineral populations between proximal and medial facies (Fig. 10). The heavy minerals within the K4 Formation are predominantly ilmenite, rutile hornblende, apatite, and zircon, with trace amounts of garnet, amphiboles and clinopyroxenes.

To identify which heavy minerals are associated with each other within the detrital succession, and therefore likely to define a unique or distinct provenance, the Pearson corelation coefficient was calculated between each mineral pair (Table 3, Fig. 10). In theory, if the abundance between two minerals is strongly correlated, it then suggests they may define a provenance and their abundances link back to a shared source region (Akinlotan et al., 2021; Aubrecht et al., 2017). Within the Kerrouchen Basin, the following mineral pairs show a correlation score above 0.4, implying a moderate or strong correlation.

The first is a metamorphic provenance, defined by elevated levels of both amphibole and clinopyroxenes. The second provenance is defined by the elevated levels of hornblende and tourmaline, which are both minerals commonly found as accessory minerals in a range of igneous and metamorphic rocks. The final provenance is defined by ultrastable heavy minerals, rutile, zircon, and ilmenite, which could be indicative of reworked sedimentary or first cycle contributions from metamorphic or igneous crustal units.

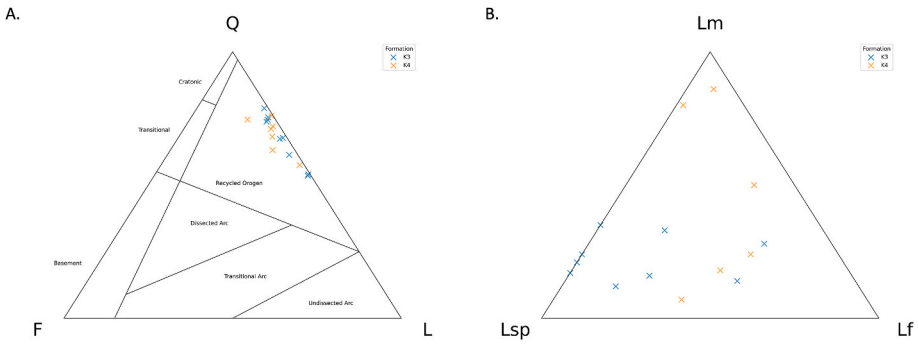

Fig. 8. (A) QFL diagram for thin sections from the Kerrouchen Basin within this study. Sediment is generally mature, with a significant proportion of quartz and lithic fragments, with low levels of feldspar, indicating a recycled orogenic provenance. (B) Lithic type fragments ternary diagram. The lithic type discrimination indicates a divergence between the K3 and K4 Formations. The K4 Formation contains higher levels of metamorphic and plutonic fragments, whereas the K3 Formation is dominated by greater levels of sedimentary and plutonic lithic fragments.

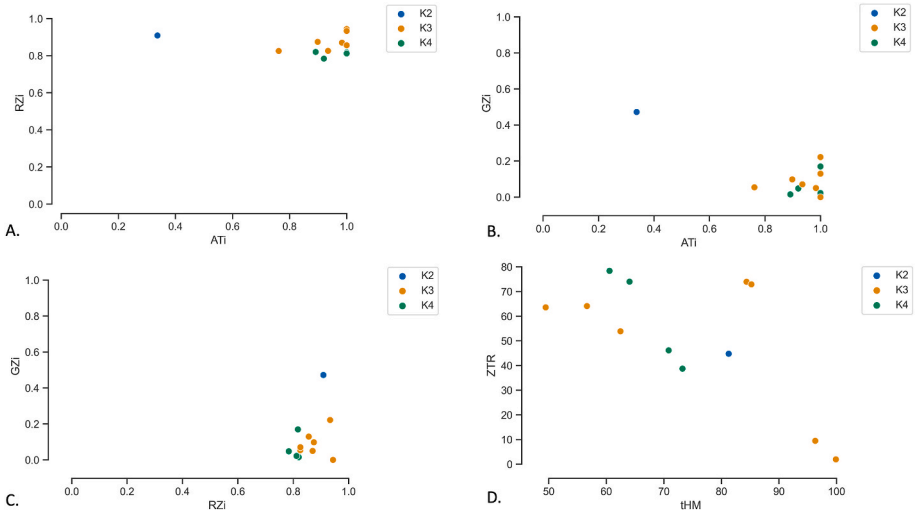

Fig. 9. Heavy Mineral Ratios for the Kerrouchen Basin do not show significant shifts in provenance between the K3 and K4 Formations. However, the Zircon– Tourmaline – Rutile vs transparent Heavy Minerals plot (D) does indicate the K3 Formation has a lower degree of ultrastable heavy minerals (ZTR) in parts than other samples. The decrease in sediment maturity within the K3 Formation indicates that the K3 Formation was sourced in part from a igneous, first cycle source region, in contrast to other samples from the K3 and K4 Formations. **Key:** GZi (Garnet: Zircon index), RZi (Rutile: Zircon index), ATi (Apatite: Tourmaline index), ZTR (Zircon Tourmaline Rutile), tHM (transparent Heavy Minerals).

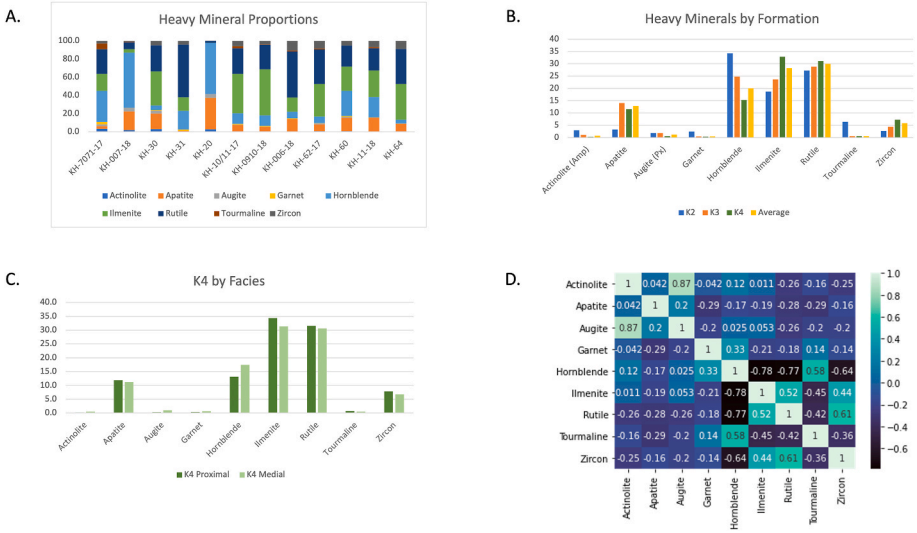

Fig. 10. The distribution of heavy minerals by Formation and facies within the Kerrouchen basin (A–C) with a correlation matrix between heavy minerals (D). Graph B indicates that hornblende varies drastically between the localities within the K3 Formation. The elevated levels of hornblende, and lowered levels of ilmenite and rutile, indicates a change in source region from an ultrastable dominated to a igneous dominated source. Graph C shows a high degree of similarity within the K4 Formation between the proximal and medial facies. This indicates a single source was feeding into the K4 system. Graph D indicates the correlation coefficient between each heavy mineral pair, allowing us to define the following provenances: Ilm + Rt + Zrn, Hb + Tur and amphiboles + pyroxenes.

7. Discussion

The combination of facies and provenance analysis of the Kerrouchen basin allows for identification and discrimination between local and regional drainage networks (Fig. 13). Firstly, field and paleoflow data indicate the presence of an axial fluvial system, the K3 Formation, and transverse alluvial-fluvial systems, the K4 Formation. Within the K3 Formation, paleoflows indicate that sediment was predominantly transported from south-west to north-east, parallel to the rift axis. The facies in the K3 Formation indicate the depositional style of this system was a braided – meandering type fluvial system. Within the K4 Formation, paleoflows are more varied, from SSW to NNE, with indicative of a tributary fluvial system feeding into the Kerrouchen Basin through relay zones within the ASMA.

The petrographic analysis indicates a broad overlap between the provenance of the axial and transverse systems; with a higher proportion of metamorphic detritus in the K4 Formation and higher levels of igneous detritus within the K3 Formation. The heavy mineral analysis suggests that the K4 Formation was sourced primarily from the ultrastable provenance, indicating either a reworked sedimentary or first cycle metamorphic or igneous source (Garzanti and Andò, 2007). The K3 Formation records two distinct provenances. The most dominant provenance is the ultrastable provenance, with a significant secondary provenance from the hornblende rich source, with additional contributions from the amphibole-clinopyroxene source, in the younger K3 section, exposed near Lenda Village. However, the outcrops near Lenda are structurally complex, with a series of thrust faults deforming the outcrop, rendering the exact relative stratigraphy within the K3 Formation unclear (Laville et al., 1995; Lorenz, 1976).

Classical models of continental rift basin tectono-sedimentary evolution suggest that axial, braided-meandering fluvial systems typically develop in open drainage basins during the normal fault arrays interaction and linkage stage (Gawthorpe and Leeder, 2000; Leeder and Gawthorpe, 1987). Consequently, the development of these axial fluvial systems is responsible for delivery of extrabasinal material to the basin and linked to growth of regional drainage networks. The appearance within the K3 Formation of evidence for an increasingly igneous rich source region – as opposed to the sedimentary and metamorphic source regions recorded by the locally draining K4 Formation (discussed below) – indicates the K3 Formation was eventually linked to an external source region and regional drainage network. Paleoflow data indicates this source region eroded by the regional drainage network was situated to the south-west of the Kerrouchen basin.

Low Temperature Thermochronology (LTT) studies help elucidate the potential source regions, identifying uplifted source regions and sinks during the initial Triassic break-up of the Pangean supercontinent.

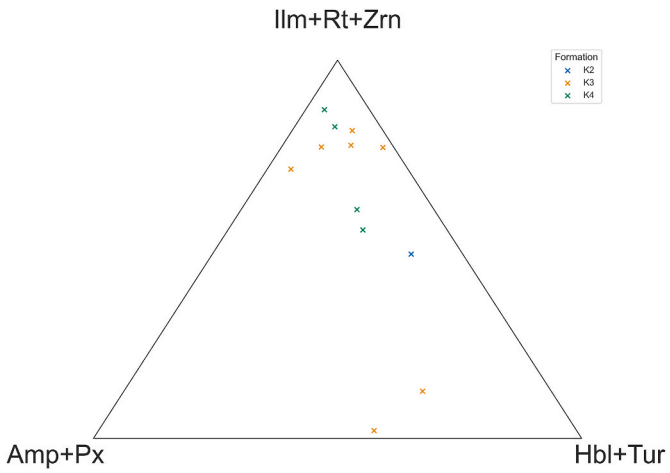

Fig. 11. Ternary diagram showing the three end member provenances identified from the correlation matrix. The ultrastable provenance (ilmenite (Ilm), rutile (Rt) and zircon (Zrn)) dominates the K4 and K3 Formation. Two samples from the K3 Formation contain elevated levels of (hornblende (Hbl) and tourmaline (Tur), indicating an igneous provenance. All samples show low values for amphibole (Amp) and pyroxene (Px).

Within the Middle – Late Triassic, three areas have been identified by thermochronology to be undergoing exhumation, the Zaer and Jebilet Massif within the Western Meseta, the Boarfa region in the eastern High Atlas and the Anti-Atlas and Reguibat Shield to the south (Barbero et al., 2007; Charton et al., 2021, 2018; Domènech et al., 2018; Gouiza et al., 2019, 2017; Lafforgue, 2016, chap. 4; Oukassou et al., 2013; Saddiqi et al., 2009). The paleoflow evidence indicating the regional drainage network was sourced to the SSW of the Kerrouchen Basin suggests that the Anti-Atlas is the most likely source region for the K3 Formation.

Within the Triassic rift basins of the Central and Western High Atlas (Oukaïmeden and Tizi-n-Test and Argana), large scale, axial fluvial systems have been identified from field and outcrop data, within the F5 and T6 sandstone units, of Middle – Late Triassic age (Bouabdelli and Piqué, 1996; Brown, 1980; Fabuel-Perez et al., 2009; Mader, 2005; Mader et al., 2017; Olsen et al., 2000). Despite the lithological and chronological overlap between the fluvial systems of the western and central high atlas, paleoflow data suggests they were not linked, with the Tizi-n-Test and Argana Basins showing a dominant axial drainage to the west, with the dominant drainage in the Oukaïmeden Basin towards the north-east (Baudon et al., 2009; Fabuel-Perez et al., 2009; Mader, 2005). This drainage divide occurs across the Toubkal Massif and Ouzellarh Salient, a Precambrian-Palaeozoic basement promontory within the Marrakech High Atlas, which played a key role within the structural evolution of the Triassic rift basins within the Atlasic domain (Domènech et al., 2018; 2015). The Ouzellarh Salient is found between the Oukaïmeden and Tizi-n-Test Triassic rift basins and divides the Atlas rift into a western (Atlantic) segment and eastern (Tethyan) segment.

Provenance studies within the High Atlas Triassic rift basins have focused primarily upon detrital zircon geochronology (Domènech et al., 2018; Marzoli et al., 2017; Perez et al., 2019). These studies have found a similar provenance for sediments either side of the Ouzallarh drainage divide, with sediment primarily sourced from Pan-African (0.6–0.85 Ga) and Eburnean (1.8–2.2 Ga) basement units present within the Western Anti-Atlas. An increased proportion of Archean grains within the Carnian period has been used to argue for expansion of drainage networks, reaching south to the Reguibat Shield (Perez et al., 2019), however a statistical review of Moroccan detrital zircon data suggests these zircon populations may not be provenance diagnostic due to extensive Phanerozoic sedimentary recycling (Lovell-Kennedy et al., 2023). When combining the regional distribution of braided-meandering, axial fluvial systems within the Moroccan Triassic rift basins with low temperature thermochronology and provenance datasets, a model can be proposed for the evolution of the Atlasic rifting during the early break-up of the Pangean supercontinent (Fig. 14).

During Triassic rifting, Variscan faults were extensively reactivated to form the Mesozoic rift basins (Domènech et al., 2018; Laville et al., 1995; Ouarhache et al., 2012). Initial, Lower-Middle Triassic sedimentation was dominated by erosion from footwall scarps, forming the basal

Table 3
Pearson correlation coefficients of pairs of heavy minerals from samples across the Kerrouchen Basin. Amp: Amphibole, Cpx: Clinopyroxene, Zrn: Zircon, Rt: Rutile, Hbl: Hornblende, Tur: Tourmaline, Ilm: Ilmenite.

Heavy mineral pair	Correlation coefficient	Degree of correlation
Amp – Cpx	0.87	Strong positive
Zrn – Rt	0.61	Moderate positive
Hbl – Tur	0.58	Moderate positive
Ilm – Rt	0.52	Moderate positive
Ilm – Zrn	0.44	Weak positive

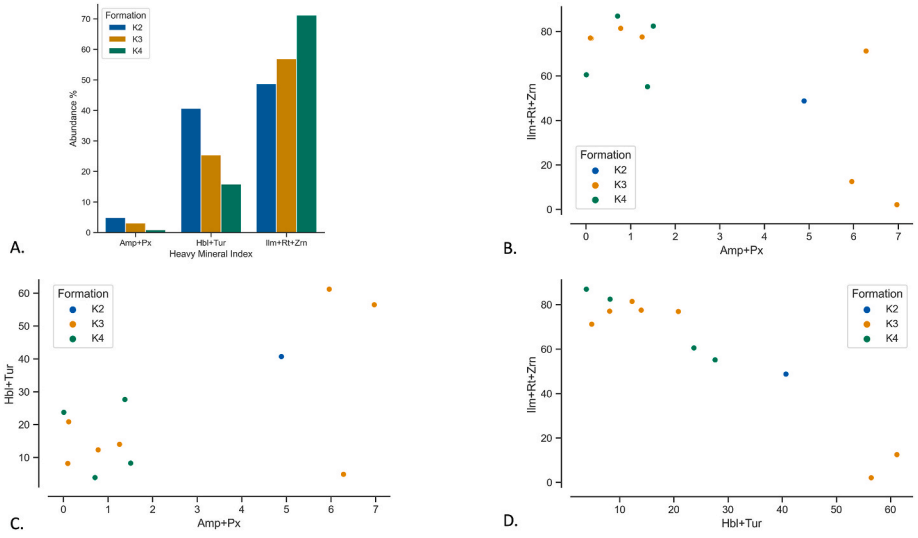

Fig. 12. Diagrams indicating the distribution of the three end member provenances of the Kerrouchen Basin. The K3 Formation contains elevated levels of amphiboles, pyroxenes, hornblendes and tourmalines relative to the K4 Formation, indicating a different source region. The heavy minerals within the K3 Formation indicate an igneous provenance, whereas the K4 Formation contains ultrastable heavy minerals indicating a recycled orogenic provenance.

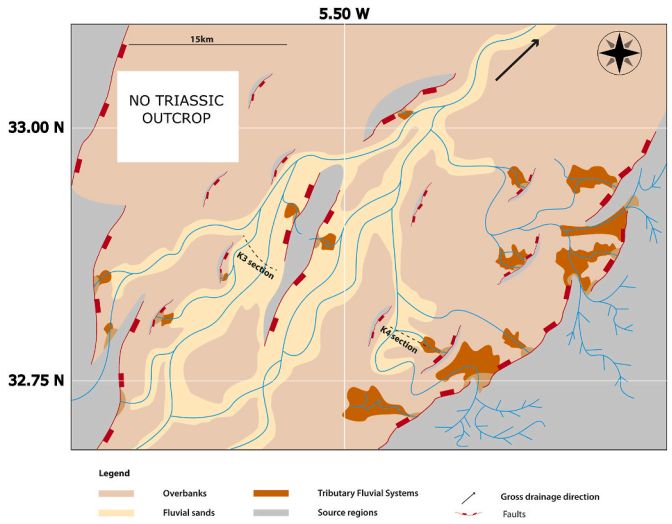

Fig. 13. Kerrouchen Basin GDE map during the Carnian rifting (ca. 230 Ma). An axial fluvial system (K3 Formation) flowed parallel to the rift basin axis, from the SSW towards the NNE. This resulted in the deposition of fluvial sands across the basin, but primarily along the basin axis. Tributary Fluvial Systems (TFS) flowed from uplifted footwall scarps, primarily to the west. These TFS are sourced from erosion into the uplifted basement, eroding through sedimentary and low-grade metamorphic units. The axial system is sourced from a region to the south (not shown), shown on Fig. 14. Logged and sampled sections (Figs. 3 and 4) are shown by dashed lines. The absence of Triassic outcrop within the north-eastern segment of the basin hampers GDE reconstructions in this region.

conglomeratic sections identified across the region (K2 Formation, Kerrouchen Basin, the F3 Formation within the Central High Atlas and the T3 Formation within the Argana Valley). During the Late Triassic axial fluvial systems developed across the Atlas rift, indicating that the Triassic rift basins were likely exorheic, with through drainage (Gawthorpe and Leeder, 2000; Leeder and Gawthorpe, 1987; Greg H Mack and Leeder, 1999). These axial drainage networks were divided into two by the Ouzellarh salient, with a western and eastern segment.

Within the eastern segment, sediment entered the Atlas rift within the Oukaïmeden basin, flowing north-east, parallel to the regional fault trend. The Kerrouchen Basin is along this fault trend, situated to the north-east of Oukaïmeden and the Ouzellarh salient. Provenance analysis indicates that basins to the east of the salient, and specifically the Oukaïmeden and Kerrouchen basins, were potentially linked by a regional drainage system during the Upper Triassic. They both share a similar paleoflow from the SSW. The axial fluvial system (K3) within the Kerrouchen Basin shows a unique provenance when compared to the transverse alluvial-fluvial fan system (K4). The provenance signal within the K3 Formation also evolves, with igneous detritus becoming more common in younger sections. Within the Oukaïmeden F5 sandstone, detrital zircon geochronology also displays a stratigraphic trend of upwards increasing levels of Archean zircons indicating an expansion of the source region during the Carnian period (Perez et al., 2019). The stratigraphic evolution of the provenance signals, recorded by both geochronology and heavy mineral analysis, indicate an expansion of the regional drainage networks within the Carnian within both the High and Middle Atlas. Taken together, the lithostratigraphic analysis, the paleoflow evidence and provenance trends indicate that the Kerrouchen Basin K3 Formation was linked to a regional drainage network sourced in the Western Anti-Atlas, feeding into the Atlas rift in Oukaïmeden and flowing north-east, through the Kerrouchen Basin towards the Tethys.

The Kerrouchen Basin also preserves a significant local drainage network, in facies observed in the K4 Formation. Sedimentary analysis, paleoflow data and provenance analysis all indicate the K4 Formation provenance was from the uplifted rift margin of the Kerrouchen Basin. A local drainage network was sourced from uplifted Palaeozoic basement to the east (Laville et al., 2004; Lorenz, 1976). Sediment was eroded from regionally metamorphosed metamorphic basement and its sedimentary cover and transported SW into the Kerrouchen Basin through relay zones within the basin margin ANMA fault. The local drainage network was an important contribution to the sediment flux within the Kerrouchen Basin and likely provided detritus that was incorporated into the axial fluvial system through erosion and reworking from the toes of alluvial-fluvial fans within the basin.

8. Conclusions

The Moroccan Triassic rift basins record a thick continental sequence, following the early break up of Pangea. The basins can be separated into two rift systems, with a drainage divide subdividing drainage ultimately into the Atlantic and Tethys. The continental sequences provide a key record of rift evolution during this key period of Earth's history. Our study focused on the sedimentology and provenance of sediments within the understudied Kerrouchen Basin of the Middle

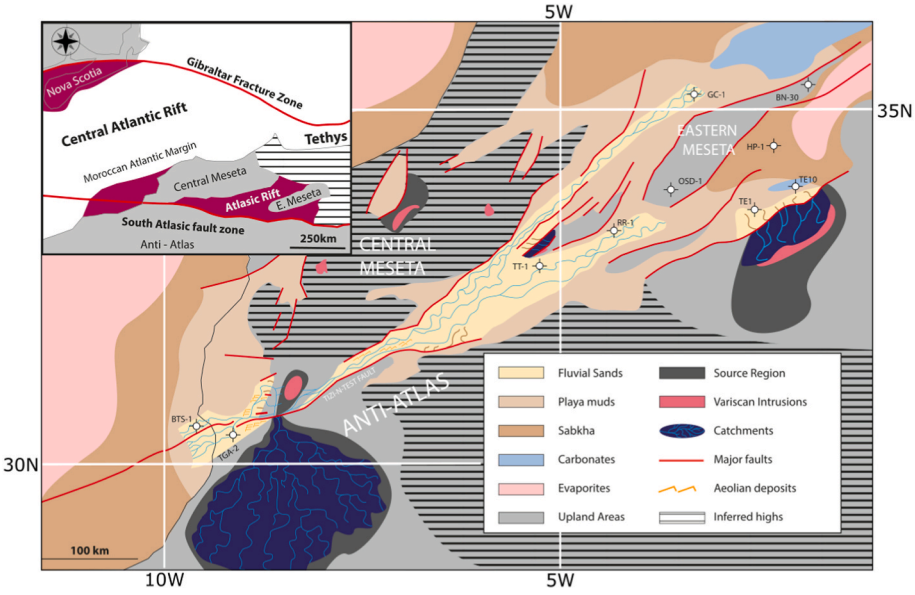

Fig. 14. Paleogeographic reconstruction of Morocco during the Carnian, ca. 230 Ma. Exhumation in the Anti-Atlas and Reguibat Shield to the south-west, and in the Plaine de Tamlelt in the east. The uplift of the Western Anti-Atlas as the rift shoulder of the Atlas rifting led to development of fluvial systems draining west towards the Atlantic, and north-east towards the Tethys. A significant drainage divide existed, separating the Atlas rift into two distinct drainage networks. Adapted from Laville et al., 2004), Fig. 1, Charton et al., 2021, Fig. 14.

High Atlas.

The fluvial clastic sedimentation that dominates the Triassic succession of the Kerrouchen Basin to record two styles of fluvial system, an axial, braided-meandering type, fluvial system, and a transverse, tributary fluvial system. The distinct fluvial styles and paleoflow directions indicate these two systems record distinct drainage networks.

Provenance analysis shows that the transverse tributary fluvial system (recorded in the K4 Formation) was primarily sourced from sedimentary to low-medium grade metamorphic units exposed in the uplifted rift shoulder of the Kerrouchen Basin and represents a local drainage network. The axial fluvial system (recorded in the K3 Formation) was primarily sourced from sedimentary and igneous units, with an increase in the proportion of igneous detritus over time. The axial position, paleoflow parallel to the rift axis and provenance signal all indicate the FA 3 (recorded in the K3 Formation) was sourced from an extrabasinal region and represents a regional drainage network.

The identification and classification of the multiple depositional systems present within the Moroccan Triassic has important implications for reservoir exploration within Morocco. Based on the model developed from the Kerrouchen Basin observations, high quality reservoirs are predicted to be present within hanging wall, running parallel to the rift axis and regional faults in the rift systems. Transverse, locally sourced TFS depositional systems, are likely to be associated with the basin bounding faults, transverse systems entering near relay zones and decreasing in reservoir quality towards the rift axis.

In conclusion, the Kerrouchen Basin preserves an example of the interaction between local and regional drainage networks within an Upper Triassic rift basin. The Kerrouchen succession offers insight into both the distribution of facies within a broad Triassic rift basin and the size of drainage networks which sourced the extensive fluvial sands found across North Africa during the Triassic.

Declaration of competing interest

The authors declare that they have no known competing financial interests or personal relationships that could have appeared to influence the work reported in this paper..

Data availability

Data will be made available on request.

Acknowledgements

This paper was part of a PhD project undertaken at the University of Manchester and funded by the North Africa Research Group and sponsoring companies. The authors would like to thank ONHYM for the logistical and scientific support in the field. The authors acknowledge and thank Ian Mounteney, Max Casson, Aude Duval-Arnauld, Orrin Bryers, Selin Coskun and Lauren O'Connor for helpful comments and discussion. Finally, the authors thank Paul Goodrich and Angel Arentegui for support in the field.

1. Appendix

Appendix 1. Heavy mineral data

Mineral Name	Basin	Formation	Actinolite	Apatite	Augite	Garnet	Hornblende	Ilmenite	Rutile	Tourmaline	Zircon	Total
KH-10/11-17	Kerrouchen	K3	0.04	0.71	0.09	0.03	1.22	4.46	2.90	0.22	0.61	10.28
KH-110/111-17	Kerrouchen	Permian	0.01	0.22	0.01	0.07	4.99	0.19	0.37	0.61	0.05	6.54
KH-7071-17	Kerrouchen	K2	0.03	0.03	0.02	0.02	0.30	0.16	0.24	0.06	0.02	0.87
KH-62-17	Kerrouchen	K4	0.03	0.46	0.06	0.01	0.44	2.15	2.28	0.06	0.50	5.99
KH-11-18	Kerrouchen	K4	0.00	2.19	0.00	0.05	3.18	4.14	3.49	0.19	0.96	14.20
KH-0910-18	Kerrouchen	K3	0.03	0.53	0.05	0.04	1.20	5.18	2.77	0.06	0.40	10.26
KH-007-18	Kerrouchen	K3	0.12	1.24	0.25	0.00	3.70	0.23	0.47	0.02	0.07	6.09
KH-006-18	Kerrouchen	K3	0.01	2.83	0.01	0.17	1.47	3.19	10.34	0.20	2.18	20.39
KH-60	Kerrouchen	K4	0.50	14.00	0.80	1.00	26.10	25.30	21.90	0.00	4.90	94.50
KH-64	Kerrouchen	K4	0.30	8.20	0.40	0.20	3.80	38.90	38.00	0.00	8.80	98.60
KH-20	Kerrouchen	K3	2.40	31.70	4.00	0.00	51.80	0.10	1.70	0.00	0.10	91.80
KH-30	Kerrouchen	K3	2.80	16.50	3.30	0.70	4.70	36.50	28.00	0.00	4.70	97.20
KH-31	Kerrouchen	K3	0.10	0.80	0.00	1.00	17.60	12.50	49.00	0.00	3.50	84.50

Appendix 2. Petrographic data

Sample	Basin	Locality	Formation	Qm	Qp	Lm	Lv	Lsp	Lsc	Lf	K-fds	Q	F	L	Total
KH-005-18	Kerrouchen	Lenda	K3	300	20	16	4	47	14	24	5	320	5	81	406
KH-008-18	Kerrouchen	Lenda	K3	242	18	12	7	90	8	16	9	260	9	117	386
KH-010-18	Kerrouchen	Lenda	K3	278	6	33	1	45	9	20	9	284	9	88	381
KH-011-18	Kerrouchen	Kerrouchen	K4	254	27	86	0	14	1	8	8	281	8	101	390
KH-012-18	Kerrouchen	Kerrouchen	K4	281	20	80	0	12	1	2	2	301	2	93	396
KH-10-17	Kerrouchen	Lenda	K3	227	60	17	18	33	22	0	12	287	12	90	389
KH-11-17	Kerrouchen	Lenda	K3	214	87	35	16	34	6	0	7	301	7	91	399
KH-20-17	Kerrouchen	Lenda	K3	234	34	24	25	44	30	0	5	268	5	123	396
KH-22-17	Kerrouchen	Lenda	K3	189	25	14	47	40	25	51	9	214	9	126	349
KH-30-17	Kerrouchen	Lenda	K3	176	12	28	65	32	33	52	2	188	2	158	348
KH-33-17	Kerrouchen	Lenda	K3	194	20	21	66	34	61	0	4	214	4	182	400
KH-40-17	Kerrouchen	Kerrouchen	K4	203	4	50	26	43	29	38	5	207	5	148	360
KH-50-17	Kerrouchen	Kerrouchen	K4	187	10	20	32	25	3	111	12	197	12	80	289
KH-60-17	Kerrouchen	Kerrouchen	K4	198	23	24	62	14	6	50	23	221	23	106	350
KH-61-17	Kerrouchen	Kerrouchen	K4	228	25	18	24	36	14	44	11	253	11	92	356
KH-62-17	Kerrouchen	Kerrouchen	K4	240	30	7	11	34	10	38	30	270	30	62	362

References

Acheche, M.H., M'rabet, A., Ghariani, H., Ouahchi, A., Montgomery, S.L., 2001. Ghadames basin, southern Tunisia: a reappraisal of Triassic reservoirs and future prospectivity. AAPG Bull. 85 (5), 765–780.

Akinlotan, Oladapo O., Rogers, Gareth H., Okunuwadje, Sunday E., 2021. Provenance evolution of the English Lower Cretaceous Weald Basin and implications for palaeogeography of the northwest European massifs: constraints from heavy mineral assemblages. Mar. Petrol. Geol. 127, 104953.

Allary, A., Andrieux, J., Lavenu, A., Ribeyrolles, M., 1972. Les nappes hercyniennes de la Meseta sud-orientale (Maroc central), vol. 274. Comptes Rendus de l'Academie des Sciences, Paris, pp. 2284–2287.

Aubrecht, R., Sýkora, M., Uher, P., Li, X.H., Yang, Y.H., Putiš, M., Plašienka, D., 2017. Provenance of the Lunz formation (Carnian) in the western Carpathians, Slovakia: heavy mineral study and in situ LA–ICP–MS U–Pb detrital zircon dating. Palaeogeogr. Palaeoclimatol. Palaeoecol. 471, 233–253.

Barbero, L., Teixell, A., Arboleya, M.L., Río, P.D., Reiners, P.W., Bougadir, B., 2007. Jurassic-to-present thermal history of the central High Atlas (Morocco) assessed by low-temperature thermochronology. Terra. Nova 19 (1), 58–64.

Barbero, Luis, Jabaloy, A., Gómez-Ortiz, D., Pérez-Peña, J.V., Rodríguez-Peces, M.J., Tejero, R., Estupiñán, J., Azdimousa, A., Vázquez, M., Asebriy, L., Barbero, L., Jabaloy, A., Gómez-Ortiz, D., Pérez-Peña, J.V., Rodríguez-Peces, M.J., Tejero, R., Estupiñán, J., Azdimousa, A., Vázquez, M., Asebriy, L., 2011. Evidence for surface uplift of the Atlas Mountains and the surrounding peripheral plateaux: combining apatite fission-track results and geomorphic indicators in the Western Moroccan Meseta (coastal Variscan Paleozoic basement). Tectonophysics 502, 90–104.

Baudon, C., Fabuel-Perez, I., Redfern, J., 2009. Structural style and evolution of a Late Triassic rift basin in the Central High Atlas, Morocco: controls on sediment deposition. Geological Journal 44(6),, 677–691.

Baudon, C., Redfern, J., Van Den Driessche, J., 2012. Permo-Triassic structural evolution of the Argana Valley, impact of the Atlantic rifting in the High Atlas, Morocco. Journal of African Earth Sciences 65, 91–104.

Beauchamp, J., 1988. Triassic sedimentation and rifting in the High Atlas (Morocco). In: Developments in geotectonics, (Vol. 22,. Elsevier, pp. 477–497.

Beauchamp, W., Barazangi, M., Demnati, A., Alji, M.E., 1996. Intracontinental rifting and inversion: Missour basin and Atlas mountains, Morocco. AAPG bulletin 80 (9), 1459–1481.

Bouabdelli, M., Piqué, A., 1996. Du bassin sur décrochement au bassin d'avant-pays: dynamique du Bassin d'Azrou-Khénifra (Maroc hercynien central). J. Afr. Earth Sci. 23 (2), 213–224.

Bourquin, S., Eschard, R., Hamouche, B., 2010. High-resolution sequence stratigraphy of Upper Triassic succession (Carnian–Rhaetian) of the Zarzaitine outcrops (Algeria): a model of fluvio-lacustrine deposits. J. Afr. Earth Sci. 58 (2), 365–386.

Brown, R.H., 1980. Triassic rocks of Argana Valley, southern Morocco, and their regional structural implications. AAPG Bulletin 64 (7), 988–1003.

Charton, R., Bertotti, G., Arantegui, A., Bulot, L., 2018. The Sidi Ifni transect across the rifted margin of Morocco (Central Atlantic): vertical movements constrained by low-temperature thermochronology. J. Afr. Earth Sci. 141, 22–32.

Charton, R., Bertotti, G., Arnould, A.D., Storms, J.E., Redfern, J., 2021. Low-temperature thermochronology as a control on vertical movements for semi-quantitative source-to-sink analysis: a case study for the Permian to Neogene of Morocco and surroundings. Basin Res. 33 (2), 1337–1383.

Courel, L., Salem, H.A., Benaouiss, N., Et-Touhami, M., Fekirine, B., Oujidi, M., Soussi, M., Tourani, A., 2003. Mid-triassic to early Liassic clastic/evaporitic deposits over the Maghreb platform. Palaeogeogr. Palaeoclimatol. Palaeoecol. 196 (1–2), 157–176.

Cousminer, H.L., Manspeizer, W., 1976. Triassic pollen date Moroccan High Atlas and the incipient rifting of Pangea as middle Carnian. Science 191 (4230), 943–945.

Dickinson, W.R., 1970. Interpreting detrital modes of graywacke and arkose. J. Sediment. Res. 40 (2), 695–707.

Domènech, M., Stockli, D.F., Teixell, A., 2018. Detrital zircon U–Pb provenance and palaeogeography of Triassic rift basins in the Marrakech High Atlas. Terra. Nova 30 (4), 310–318.

Domènech, M., Teixell, A., Stockli, D.F., 2016. Magnitude of rift-related burial and orogenic contraction in the Marrakech High Atlas revealed by zircon (U-Th)/He thermochronology and thermal modeling. Tectonics 35 (11), 2609–2635.

El Arabi, EH, Ferrandini, J, Essamoud, R, 2003. Triassic stratigraphy and structural evolution of a rift basin: the Ec Cour basin, High atlas of Marrakech, Morocco. Journal of African Earth Sciences 36 (1–2), 29–39.

Ellouz, N., Patriat, M., Gaulier, J.M., Bouatmani, R., Sabounji, S., 2003. From rifting to Alpine inversion: mesozoic and Cenozoic subsidence history of some Moroccan basins. Sediment. Geol. 156 (1–4), 185–212.

Escosa, F.O., Leprêtre, R., Spina, V., Gimeno-Vives, O., Kergaravat, C., Mohn, G., de Lamotte, D.F., 2021. Polyphased mesozoic rifting from the Atlas to the north-west Africa paleomargin. Earth Sci. Rev. 220, 103732.

Fabuel-Perez, I., Redfern, J., Hodgetts, D., 2009. Sedimentology of an intra-montane rift-controlled fluvial dominated succession: the upper Triassic Oukaimeden sandstone formation, central high atlas, Morocco. Sediment. Geol. 218 (1–4), 103–140.

Fiechtner, L., Friedrichsen, H., Hammerschmidt, K., 1992. Geochemistry and geochronology of early mesozoic tholeiites from Central Morocco. Geol. Rundsch. 81, 45–62.

Galeazzi, S., Point, O., Haddadi, N., Mather, J., Druesne, D., 2010. Regional geology and petroleum systems of the Illizi–Berkine area of the Algerian Saharan Platform: an overview. Mar. Petrol. Geol. 27 (1), 143–178.

Galeazzi, S., Point, O., Haddadi, N., Mather, J., Druesne, D., 2012. The Illizi and Berkine basins in southern Algeria. In: Regional Geology and Tectonics: Phanerozoic Passive Margins, Cratonic Basins and Global Tectonic Maps. Elsevier, pp. 662–729.

Galehouse, J.S., 1971. Point Counting. *Procedures in Sedimentary Petrology*.

Garzanti, E., Andò, S., 2007. Plate tectonics and heavy mineral suites of modern sands. Dev. Sedimentol. 58, 741–763.

Garzanti, E., Vezzoli, G., 2003. A classification of metamorphic grains in sands based on their composition and grade. J. Sediment. Res. 73 (5), 830–837.

Garzanti, E., Resentini, A., Vezzoli, G., Ando, S., Malusa, M.G., Padoan, M., Paparella, P., 2010. Detrital fingerprints of fossil continental-subduction zones (axial belt provenance, European Alps). J. Geol. 118 (4), 341–362.

Gawthorpe, R.L., Leeder, M.R., 2000. Tectono-sedimentary evolution of active extensional basins. Basin Res. 12 (3-4), 195–218.

Gouiza, M., Charton, R., Bertotti, G., Andriessen, P., Storms, J.E.A., 2017. Post-Variscan evolution of the Anti-Atlas belt of Morocco constrained from low-temperature geochronology. Int. J. Earth Sci. 106, 593–616.

Gouiza, M., Bertotti, G., Charton, R., Haimoudane, K., Dunkl, I., Anczkiewicz, A.A., 2019. New evidence of 'Anomalous' vertical movements along the Hinterland of the Atlantic NW African margin. J. Geophys. Res. Solid Earth 124 (12), 13333–13353.

Hafid, M., 2000. Triassic–early Liassic extensional systems and their Tertiary inversion, Essaouira Basin (Morocco). Marine and Petroleum Geology 17 (3), 409–429.

Hmich, D., Schneider, J.W., Saber, H., Voigt, S., El Wartiti, M., 2006. New continental Carboniferous and Permian faunas of Morocco: implications for biostratigraphy, palaeobiogeography and palaeoclimate. Geological Society, London, Special Publications 265 (1), 297–324.

Hoepffner, C., 1987. La tectonique hercynienne dans l'Est du Maroc. Doctoral dissertation, Université Louis Pasteur).

Hoepffner, C., Soulaimani, A., Piqué, A., 2005. The moroccan hercynides. J. Afr. Earth Sci. 43 (1–3), 144–165.

Hoepffner, C., Houari, M.R., Bouabdelli, M., 2006. Tectonics of the North African Variscides (Morocco, western Algeria): an outline. Compt. Rendus Geosci. 338 (1–2), 25–40.

Hubert, J.F., 1962. A zircon-tourmaline-rutile maturity index and the interdependence of the composition of heavy mineral assemblages with the gross composition and texture of sandstones. Journal of Sedimentary Research 32 (3), 440–450.

Lachkar, G., Ouarhache, D., Charriere, A., 2000. Nouvelles données palynologiques sur les formations sédimentaires associées aux basaltes triasiques du Moyen Atlas et de la Haute Moulouya (Maroc). Rev. Micropaleontol. 43 (4), 281–299.

Lafforgue, L., 2016. Place de la minéralisation de manganèse de Bouarfa dans l'évolution méso-cénozoïque de l'oriental marocain (Doctoral dissertation, Université Paris-Saclay (ComUE)).

Laville, E., Petit, J.P., 1984. Role of synsedimentary strike-slip faults in the formation of Moroccan Triassic basins. Geology 12 (7), 424–427.

Laville, E., Charroud, A., Fedan, B., Charroud, M., Pique, A., 1995. Inversion negative et rifting atlasique; l'exemple du bassin triasique de Kerrouchene (Maroc). Bull. Soc. Geol. Fr. 166 (4), 365–374.

Laville, E., Pique, A., Amrhar, M., Charroud, M., 2004. A restatement of the Mesozoic Atlasic rifting (Morocco). J. Afr. Earth Sci. 38 (2), 145–153.

Leeder, M.R., Gawthorpe, R.L., 1987. Sedimentary models for extensional tilt-block/half-graben basins. Geological Society, London, Special Publications 28 (1), 139–152.

Leleu, S., Hartley, A.J., 2010. Controls on the stratigraphic development of the Triassic fundy basin, Nova Scotia: implications for the tectonostratigraphic evolution of Triassic Atlantic rift basins. J. Geol. Soc. 167 (3), 437–454.

Leleu, S., Hartley, A.J., van Oosterhout, C., Kennan, L., Ruckwied, K., Gerdes, K., 2016. Structural, stratigraphic and sedimentological characterisation of a wide rift system: The Triassic rift system of the Central Atlantic Domain. Earth-Science Reviews 158, 89–124.

Lorenz, J., 1976. Triassic sediments and basin structure of the Kerrouchen Basin, central Morrocco. J. Sediment. Res. 46 (4), 897–905.

Lovell-Kennedy, J., Roquette, E., Schröder, S., Redfern, J., 2023. 'I hate sand… it gets everywhere'—Phanerozoic sedimentary recycling from NW Africa. Basin Res. 35 (1), 187.

Macgregor, D.S., 1998. Giant fields, petroleum systems and exploration maturity of Algeria. Geological Society, London, Special Publications 132 (1), 79–96.

Mack, G.H., Leeder, M.R., 1999. Climatic and tectonic controls on alluvial-fan and axial-fluvial sedimentation in the Plio-Pleistocene Palomas half graben, southern Rio Grande Rift. J. Sediment. Res. 69 (3), 635–652.

Mader, N.K., 2005. Sedimentology and Sediment Distribution of Upper Triassic Fluvio-Aeolian Reservoirs on a Regional Scale (Central Algeria, SW Morocco, NE Canada): an Integrated Approach Unravelling the Influence of Climate versus Tectonics on Reservoir Architecture (Doctoral Dissertation. The University of Manchester (United Kingdom)).

Mader, N.K., Redfern, J., 2011. A sedimentological model for the continental upper Triassic Tadrart Ouadou sandstone member: recording an interplay of climate and tectonics (Argana Valley; south-west Morocco). Sedimentology 58 (5), 1247–1282.

Mader, N.K., Redfern, J., El Ouataoui, M., 2017. Sedimentology of the Essaouira Basin (Meskala Field) in context of regional sediment distribution patterns during upper Triassic pluvial events. J. Afr. Earth Sci. 130, 293–318.

Martin, A.J., 2000. Flaser and wavy bedding in ephemeral streams: a modern and an ancient example. Sediment. Geol. 136 (1–2), 1–5.

Marzoli, A., Bertrand, H., Knight, K.B., Cirilli, S., Buratti, N., Vérati, C., et al., 2004. Synchrony of the Central Atlantic magmatic province and the Triassic-Jurassic boundary climatic and biotic crisis. Geology 32 (11), 973–976.

Marzoli, A., Davies, J.H., Youbi, N., Merle, R., Dal Corso, J., Dunkley, D.J., Bensalah, M. K., 2017. Proterozoic to Mesozoic evolution of North-West Africa and Peri-

Gondwana microplates: detrital zircon ages from Morocco and Canada. Lithos 278, 229–239.
Mattis, A.F., 1977. Nonmarine Triassic sedimentation, central high atlas Mountains, Morocco. J. Sediment. Res. 47 (1), 107–119.
Miall, A.D., 2013. The Geology of Fluvial Deposits: Sedimentary Facies, Basin Analysis, and Petroleum Geology. Springer.
Morton, A.C., Hallsworth, C., 1994. Identifying provenance-specific features of detrital heavy mineral assemblages in sandstones. Sedimentary Geology 90 (3–4), 241–256.
Nichols, G.J., Fisher, J.A., 2007. Processes, facies and architecture of fluvial distributary system deposits. Sediment. Geol. 195 (1–2), 75–90.
Ntarmouchant, A., Smaili, H., dos Santos, T.B., Dahire, M., Sabri, K., Ribeiro, M.L., Driouch, Y., Santos, R., Calvo, R., 2016. New evidence of effusive and explosive volcanism in the Lower Carboniferous formations of the Moroccan Central Hercynian Massif: geochemical data and geodynamic significance. J. Afr. Earth Sci. 115, 218–233.
Olsen, P.E., Kent, D.V., Fowell, S.J., Schlische, R.W., Withjack, M.O., LeTourneau, P.M., 2000. Implications of a Comparison of the Stratigraphy and Depositional Environments of the Argana (Morocco) and Fundy (Nova Scotia, Canada) Permian-Jurassic Basins.
Ouarhache, D., Charrière, A., Chalot-Prat, F., El-Wartiti, M., 2000. Sédimentation détritique continentale synchrone d'un volcanisme explosif dans le Trias terminal à infra-Lias du domaine atlasique (Haute Moulouya, Maroc)(Late Triassic to infra-Liassic continental detrital sedimentation synchronous with an explosive volcanic event in the Atlas area [Hgh Moulouya, Morocco]). J. Afr. Earth Sci. 31 (3–4), 555–570.
Ouarhache, D., Charriere, A., Chalot-Prat, F., Wartiti, M.E., 2012. Triassic to early Liassic continental rifting chronology and process at the southwest margin of the Alpine Tethys (Middle Atlas and High Moulouya, Morocco); correlations with the Atlantic rifting, synchronous and diachronous. Bull. Soc. Geol. Fr. 183 (3), 233–249.
Oujidi, M., Azzouz, O., Elmi, S., 2006. Synsedimentary tectonics of the Triassic carbonate Formation of the Oujda Mountains (eastern Meseta, Morocco): geodynamic implications. Geological Society, London, Special Publications 262 (1), 75–85.
Oukassou, M., Saddiqi, O., Barbarand, J., Sebti, S., Baidder, L., Michard, A., 2013. Post-Variscan exhumation of the Central Anti-Atlas (Morocco) constrained by zircon and apatite fission-track thermochronology. Terra. Nova 25 (2), 151–159.
Perez, N.D., Teixell, A., Gómez-Gras, D., Stockli, D.F., 2019. Reconstructing extensional basin architecture and provenance in the Marrakech High Atlas of Morocco: implications for rift basins and inversion tectonics. Tectonics 38 (5), 1584–1608.
Piqué, A., Le Roy, P., Amrhar, M., 1998. Transtensive synsedimentary tectonics associated with ocean opening: the Essaouira–Agadir segment of the Moroccan Atlantic margin. J. Geol. Soc. 155 (6), 913–928.
Redfern, J., Shannon, P.M., Williams, B.P.J., Tyrrell, S., Leleu, S., Fabuel Perez, I., et al., 2010. An integrated study of Permo-Triassic basins along the North Atlantic passive margin: implication for future exploration. In: Geological Society, London, Petroleum Geology Conference Series, vol. 7. The Geological Society of London, London, pp. 921–936. No. 1.
Ruiz, G.M.H., Sebti, S., Negro, F., Saddiqi, O., Frizon de Lamotte, D., Stockli, D., et al., 2011. From central Atlantic continental rift to Neogene uplift–western Anti-Atlas (Morocco). Terra. Nova 23 (1), 35–41.
Sabaou, N., Lawton, D.E., Turner, P., Pilling, D., 2005. Floodplain deposits and soil classification: the prediction of channel sand distribution within the Triassic Argilogreseux inferieur, Berkine Basin, Algeria. J. Petrol. Geol. 28 (3), 223–239.
Saddiqi, O., El Haimer, F.Z., Michard, A., Barbarand, J., Ruiz, G.M.H., Mansour, E.M., et al., 2009. Apatite fission-track analyses on basement granites from south-western Meseta, Morocco: paleogeographic implications and interpretation of AFT age discrepancies. Tectonophysics 475 (1), 29–37.
Sahabi, M., Aslanian, D., Olivet, J.L., 2004. A new starting point for the history of the central Atlantic. Geoscience Proceedings 336 (12), 1041–1052.
Schettino, A., Turco, E., 2009. Breakup of Pangaea and plate kinematics of the central Atlantic and Atlas regions. Geophys. J. Int. 178 (2), 1078–1097.
Soussi, M., Niedźwiedzki, G., Tałanda, M., Dróżdż, D., Sulej, T., Boukhalfa, K., et al., 2017. Middle Triassic (Anisian-Ladinian) Tejra red beds and Late Triassic (Carnian) carbonate sedimentary records of southern Tunisia, Saharan Platform: biostratigraphy, sedimentology and implication on regional stratigraphic correlations. Mar. Petrol. Geol. 79, 222–256.
Turner, P., Pilling, D., Walker, D., Exton, J., Binnie, J., Sabaou, N., 2001. Sequence stratigraphy and sedimentology of the late Triassic TAG-I (Blocks 401/402, Berkine basin, Algeria). Mar. Petrol. Geol. 18 (9), 959–981.
Van Houten, F.B., 1977. Triassic-Liassic deposits of Morocco and eastern North America: comparison. AAPG Bull. 61 (1), 79–99.
Veevers, J.J., 1994. Earth's paleoclimate and sedimentary environments. Pangea: Paleoclimate, tectonics, and sedimentation during accretion, zenith, and breakup of a supercontinent 288, 13.
Verati, C., Rapaille, C., Féraud, G., Marzoli, A., Bertrand, H., Youbi, N., 2007. 40Ar/39Ar ages and duration of the central Atlantic magmatic province volcanism in Morocco and Portugal and its relation to the Triassic–Jurassic boundary. Palaeogeogr. Palaeoclimatol. Palaeoecol. 244 (1–4), 308–325.
Whiteside, J.H., Olsen, P.E., Kent, D.V., Fowell, S.J., Et-Touhami, M., 2007. Synchrony between the central Atlantic magmatic province and the Triassic–Jurassic mass-extinction event? Palaeogeogr. Palaeoclimatol. Palaeoecol. 244 (1–4), 345–367.